Vol 18 No 11, November 2009
1674-1056/2009/18(11)/4781-05

Chinese Physics B

© 2009 Chin. Phys. Soc.
and IOP Publishing Ltd

Disappearance of isospin effect in projectile fragmentation at intermediate energy*

Ma Chun-Wang(马春旺)† Wei Hui-Ling(魏慧玲),
Wang Jun-Yang(王俊阳), and Liu Gao-Jie(刘高杰)
Department of Physics, Henan Normal University, Xinxiang 453007*, China*

(Received 7 December 2008; revised manuscript received 3 June 2009)

The 140 MeV/u ^{40,48}Ca+^{9}Be and ^{58,64}Ni+^{9}Be reactions are simulated by the statistical abrasion ablation model, and the simulation results are compared to the National Superconducting Cyclotron Laboratory (NSCL) experimental data. By comparing the fragment isotopic distributions of ^{40,48}Ca and ^{58,64}Ni, we study the isospin effect in the projectile fragmentation induced by the neutron-rich nuclei at intermediate energy experimentally and theoretically. It is found that the isospin effect in projectile fragmentation decreases and even disappears as the violence of the collision increases.

Keywords: isospin effect, projectile fragmentation, neutron-rich nucleus

PACC: 2000, 2570, 2570N

Projectile fragmentation is a well established technique for the production of rare isotope beams and is used by many radioactive ion-beam facilities in the world. The process of projectile fragmentation has been studied extensively for investigation of reaction mechanisms in heavy ion collisions at intermediate and high energies.[1−7] Understanding the physics of projectile fragmentation is important not only for rare-isotope beam production purposes but also for the fundamental nuclear physics processes involved in nuclear collisions.[1−3,8−14]

The isospin effects of various physical phenomena, such as multifragmentation, collective flow, preequilibrium nucleon emission, etc., have been reported.[6,15−22] These studies have shown that isospin effect exists in nuclear reactions induced by exotic nuclei but it may disappear under some conditions. In projectile fragmentation, the yield of neutron-rich nuclei from fragmentation of a neutron-rich projectile is larger than that from stable nuclei; this is one sign of the isospin effect in fragment production.[22−25] But the difference becomes smaller with the increase of the charge difference between the fragment and the projectile and may disappear finally. In Refs.[23] and [24], Fang *et al* have presented the fragment isotopic distributions of ^{16,18}O, ^{36,40}Ar and ^{40,48}Ca, calculated by the modified statistical abrasion ablation (SAA) model. It was found that the peak position of isotopic distributions from stable nucleus induced reactions has a shift toward the neutron-rich side as compared to that from neutron-rich nucleus induced reactions. The shift becomes larger when the difference in neutron number between the two projectiles is bigger. This phenomenon is called the isospin effect in projectile fragmentation. In Refs.[23] and [24] it was pointed out that the isospin effect of fragmentation reaction on isotopic distribution decreased with the increase of the atomic number difference and disappeared finally. But the results in Refs.[23] and [24] were based on model calculations and had no direct experimental evidence.

In Refs.[26] and [27], the measured cross sections of more than 1400 fragments produced in 140 MeV/u ^{40,48}Ca+^{9}Be/^{181}Ta and ^{58,64}Ni+^{9}Be/^{181}Ta reactions were reported. These detailed data make it possible to compare the fragment isotopic distributions of symmetric and asymmetric projectile nuclei. In this paper, the cross sections of fragments produced in the four reactions were simulated using the SAA model and compared to the experimental data. The isospin dependence of the projectile-like fragmentation was studied by comparing the fragment isotopic distributions. The experimental data used in this paper were taken from Ref.[27].

The SAA model was developed by Brohm *et al* to describe peripheral nuclear collisions at high energies

*Project partially supported by the National Natural Science Foundation of China (Grant Nos 10775168 and 10775039), Shanghai Development Foundation for Science and Technology (Grant No 06QA14062), and the State Key Program of Basic Research of China (Grant No 2007CB815004).

†Corresponding author. E-mail: machunwang@126.com

in a picture of quasi-free nucleon–nucleon collisions.[28] It was modified by Fang *et al*[23,25,29] and Zhong *et al* to study heavy ion collisions at intermediate energy.[30,31] In the SAA model, the reaction is described as a two-step process. The initial stage is described by a Glauber-type model as 'participants' and 'spectators'. The participants in an overlapping region between the projectile and the target interact strongly while the spectators are left to move almost without being disturbed.[32] In the second evaporation stage, the system reorganizes due to excitation, which means that it is de-excited and thermalized by the cascade evaporation of light particles. After the deexcitation, the results of the final fragment, which are comparable to the experimental data, are obtained. Detailed descriptions of the SAA model can be found in Refs.[14], [23], [28] and [29].

In the SAA model, the colliding nuclei are described to be composed of parallel tubes orienting along the beam direction. Neglecting the transverse motion, the collision is described by independent interactions between tube pairs. Assuming a binomial distribution for the absorbed projectile neutrons and protons in the interaction between a specific pair of tubes, the distributions of the total abraded neutrons and protons can be determined. For an infinitesimal tube in the projectile, the transmission probabilities for neutrons (protons) at a given impact parameter $\boldsymbol{b}$ are calculated by

$$t_k(\boldsymbol{s}-\boldsymbol{b}) = \exp\{-[D_n^T(\boldsymbol{s}-\boldsymbol{b})\sigma_{nk}+D_n^P(\boldsymbol{s}-\boldsymbol{b})\sigma_{pk}]\}, \quad (1)$$

where D^{T} is the nuclear-density distribution of the target integrated along the beam direction and normalized by $\int \mathrm{d}^2 s D_n^{\mathrm{T}} = N^{\mathrm{T}}$ and $\int \mathrm{d}^2 s D_p^T = Z^{\mathrm{T}}$. With N^{T} and Z^{T} referring to the neutron and proton number in the target respectively, the vectors $\boldsymbol{s}$ and $\boldsymbol{b}$ are defined in the plane perpendicular to beam, and $\sigma_{k'k}$ are the free nucleon–nucleon cross sections ($k', k = n$ for neutron and $k', k = p$ for proton). So the average absorbed mass in the limit to infinitesimal tubes at a given $\boldsymbol{b}$ is

$$\langle \Delta A(b) \rangle = \int \mathrm{d}^2 s D_n^T(\boldsymbol{s})[1 - t_n(\boldsymbol{s}-\boldsymbol{b})] + \int \mathrm{d}^2 s D_p^P(\boldsymbol{s})[1 - t_p(\boldsymbol{s}-\boldsymbol{b})]. \quad (2)$$

The excitation energy of a projectile spectator is estimated by a simple relation of $E^* = 13.3\langle \Delta A(b) \rangle$MeV, where 13.3 is a mean excitation energy due to an abraded nucleon from the initial projectile.[33] In the calculations, the free space nucleon–nucleon cross sections have been adopted and the proton and neutron density distributions have been assumed to be of Fermi-type,

$$\rho_i(r) = \frac{\rho_i^0}{1 + \exp(\frac{r-C_i}{t_i/4.4})}, \quad i = n, p, \quad (3)$$

where ρ_i^0 is the normalization constant which ensures that the integration of the density distribution equals the number of neutrons ($i = n$) or protons ($i = p$); t_i is the diffuseness parameter; C_i is half the density radius of the neutron or proton.

In Fig.1, cross section of fragments produced in ^{40,48}Ca+^{9}Be and cross section of fragments with $Z < 20$ in ^{58,64}Ni+^{9}Be are plotted. The cross sections of fragments with Z number greater than 20 of ^{58,64}Ni are not plotted because, on the one hand, the shape and trend of the fragments' isotopic distributions are similar to those of ^{40,48}Ca; on the other hand, it facilitates the comparison between fragments produced in the most central collisions of the projectile with different values of Z. It can be seen that the calculated values of σ of fragments by the SAA model reproduce the experimental data well, except those of the light fragments. This is due to the fact that we took the free space nucleus–nucleus cross section in the calculations and did not consider the in-medium effect of the nucleus–nucleus cross section.

The experimental fragment isotopic distributions of ^{40,48}Ca fragmentation verify the predictions in Refs.[23] and [24]. Roughly speaking, the peak of the isotopic distributions of ^{48}Ca shows a shift toward the neutron-rich side as compared to that of ^{40}Ca. The shift demonstrates the isospin effect in the fragmentation as explained in Refs.[23] and [24]. It can be seen that the shift decreases with the increase of the atomic number difference $Z_p - Z$ (Z_p is the proton number of the projectile nucleus). Unlike the the SAA model prediction in Refs.[23] and [24], where the isospin effect disappears at the sodium (Na) isotopes, the isospin effect does not disappear until the nitrogen (N) isotopes for the ^{40}Ca and ^{48}Ca project.

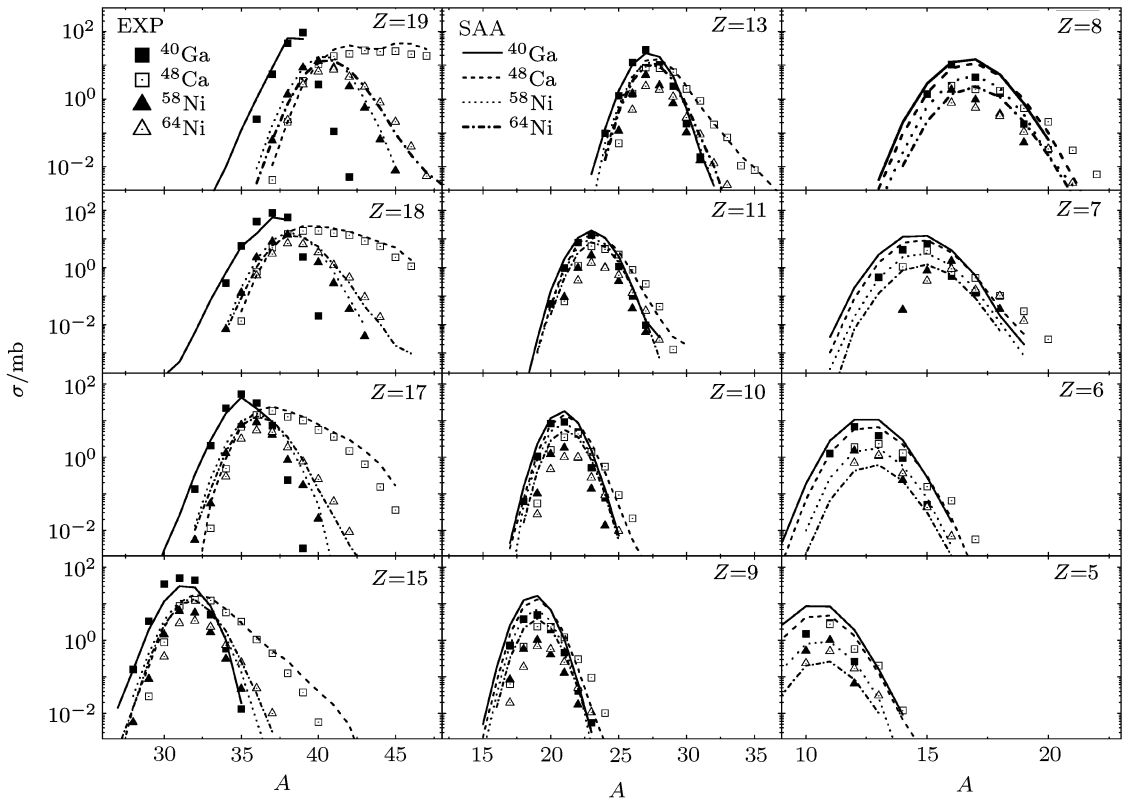


Fig.1. Cross sections of the fragments produced in 140MeV/u ^{40,48}Ca+^{9}Be and ^{58,64}Ni+^{9}Be reactions. The x axis is the mass number of fragments. The solid and open squares denote σ of fragment isotopes of ^{40}Ca and ^{48}Ca, respectively. The solid and open triangles denote the values of σ the same as those of the squares but for ^{58}Ni and ^{64}Ni. The solid and dashed lines denote the calculated values of σ of fragments of ^{40}Ca and ^{48}Ca by the SAA model, respectively. The dotted and dash dotted lines denote the calculated values of σ of fragments of ^{58}Ni and ^{64}Ni by the SAA model, respectively.

The shift from the fragment isotopic distribution of ^{58}Ni to that of ^{64}Ni and the decrease of the shift can be seen from the $Z = 19$ to the $Z = 15$ isotopes. From the aluminum ($Z = 13$) isotopes, there is little difference between the fragment isotopic distributions of ^{58}Ni and ^{64}Ni, thereby indicating the disappearance of the isospin effect.

To understand the isospin effect of the fragmentation reaction on isotopic distribution more clearly, the peak position and the peak width are extracted by a Gaussian fit to the fragment isotopic distributions. A difference parameter, $\Delta A = A_{\rm peak,asy} - A_{\rm peak,sy}$ ('asy' means the asymmetric neutron-rich projectile and 'sy' means the symmetry nucleus projectile), is defined to describe the difference in the peak position of fragment isotopic distribution between symmetric and asymmetric projectile nuclei. In Fig.2 a comparison between the experimental data and the SAA model calculations shows that the trends of ΔA of ^{40,48}Ca and ^{58,64}Ni are the same but the results of the SAA model are smaller than measurements. The widths of the Gaussian fitting show little difference between measurements and calculations. Roughly speaking, the parameter $(Z_{\rm proj} - Z)/Z_{\rm proj}$ can be viewed as a measure of the violence of the nuclear reaction which is related to the reaction time, the dissipated energy or the excitation energy and the impact parameter.[23] For the two reaction systems, and especially for ^{58,64}Ni, the values of ΔA become smaller and vary little when $(Z_{\rm proj} - Z)/Z_{\rm proj} > 0.5$, which means that central collisions dominate the reaction. Both the widths of the fragment isotopic distributions of ^{40,48}Ca and those of ^{58,64}Ni reaction systems approach a balance width when $(Z_{\rm proj} - Z)/Z_{\rm proj} > 0.5$ as predicted in Ref.[23].

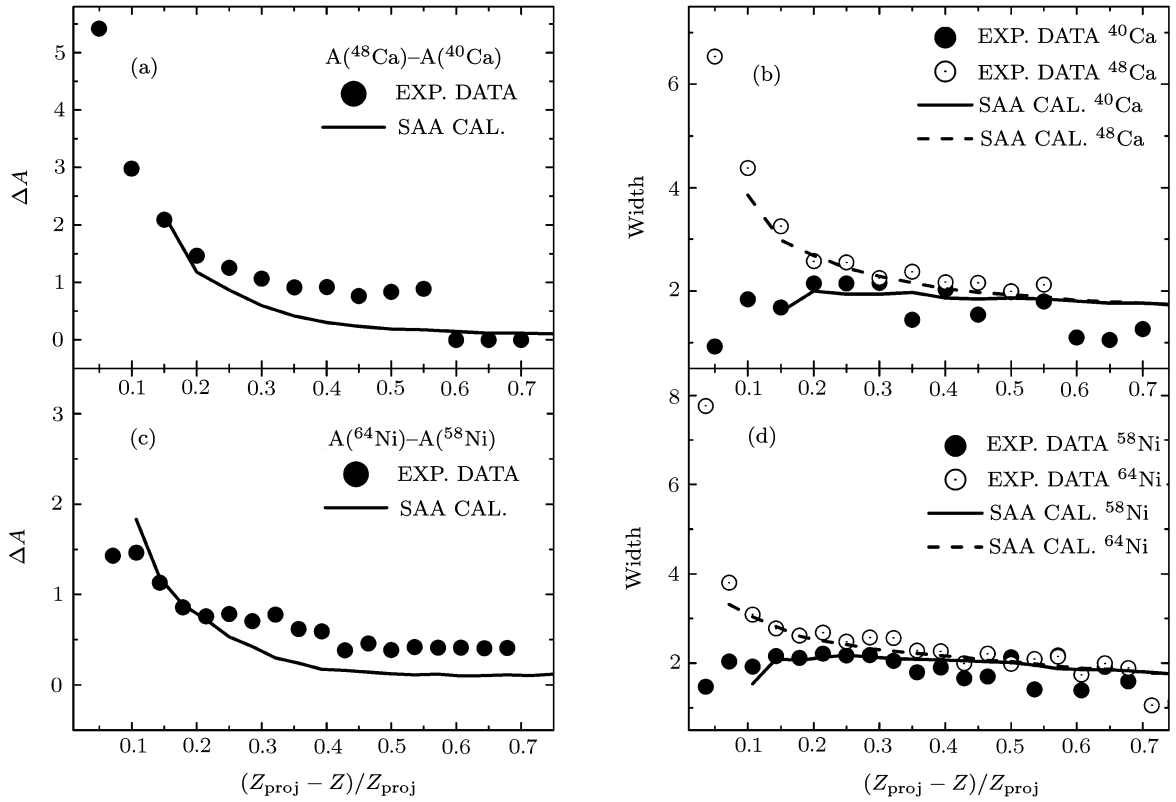


Fig.2. Results of Gaussian fit to the fragment isotopic distributions from symmetric and asymmetric projectile nuclei. (a) is for ΔA (= $A_{\rm peak}(^{48}{\rm Ca})$–$A_{\rm peak}(^{40}{\rm Ca})$) of ^{40,48}Ca as a function of $(Z_{\rm proj} - Z)/Z_{\rm proj}$. (b) is for the widths of fragment isotopic distributions by Gaussian fitting of ^{40,48}Ca as a function of $(Z_{\rm proj} - Z)/Z_{\rm proj}$. (c) is for ΔA(= $A_{\rm peak}(^{64}{\rm Ni})$–$A_{\rm peak}(^{58}{\rm Ni})$) as a function of $(Z_{\rm proj} - Z)/Z_{\rm proj}$. (d) is for the widths of fragment isotopic distributions by Gaussian fitting of ^{58,64}Ni as a function of $(Z_{\rm proj} - Z)/Z_{\rm proj}$. The open and filled dots denote the measurements and the solid and the dashed lines denote the calculations by the SAA model.

As explained in Ref.[23], for a peripheral reaction, it is dominated by the nucleon–nucleon interaction of the nuclear surface where nucleons are loosely bound and the neutron and the proton density distributions are quite different for neutron-rich nuclei. This makes the isospin effect exhibited in the fragment isotopic distribution. With the increase of $Z_{\rm proj} - Z$, roughly speaking, the impact parameter is decreasing. For the most central reaction, it is dominated by the nucleon–nucleon interaction of the more central part of the nucleon distribution where the neutron and proton density distributions have little difference. Also, the higher excitation energy in the strictly-bound matter will wash out the difference between the sequential evaporation processes of the neutron-rich and symmetric projectiles. So the isospin effect will decrease and even disappear for $(Z_{\rm proj} - Z)/Z_{\rm proj} > 0.5$.

In summary, the cross sections of fragments produced in 140 MeV/u ^{40,48}Ca+^{9}Be and ^{58,64}Ni+^{9}Be reactions have been calculated by the SAA model. The isospin effects in the projectile fragmentation have been studied by comparing the fragment isotopic distributions. The predictions in Refs.[23] and [24] have been verified experimentally and it is found that the fragment isotopic distribution shifts toward the neutron-rich side for a neutron-rich projectile, but the shift decreases with the increase of atomic number difference $Z_{\rm proj} - Z$ or the violence of the nuclear reactions. The isospin effect of the fragmentation reaction on the fragment isotopic distribution will disappear when $(Z_{\rm proj} - Z)/Z_{\rm proj}$ becomes larger than 0.5.

References

[1] Li B A, Ren Z Z, Ko C M and Yennellon S J 1996 *Phys. Rev. Lett.* **76** 4492

[2] Brown B A 2000 *Phys. Rev. Lett.* **85** 5296

[3] Tsang M B, Friedman W A, Gelbke C K, Lynch W G, Verde G and Xu H 2001 *Phys. Rev. Lett.* **86** 5023

[4] Ma Y G, Siwek A, Peter J, Gulminelli F, Dayras R, Nalpas L, Tamain B, Vient E, Auger G, Bacri Ch O, Benlliure J, Bisquer E, Borderie B, Bougault R, Brou R, Charvet J L, Chbihi A, Colin J, Cussol D, De Filippo E, Demeyer A, Dore D, Durand D, Ecomard P, Eudes P, Gerlic E, Gourio D, Guinet D, Laforest R, Lautesse P, Laville J L, Lebreton L, Lecolley J F, Le Fevre A, Lefort T, Legrain R, Lopez O, Louvel M, Lukasikd J, Marie N, Metivier V, Ouatizerga A, Parlog M, Plagnol E, Rahmani A, Reposeur T, Rivet M F, Rosato E, Saint-Laurent F, Squalli M, Steckmeyer J C, Stern M, Tassan-Got L, Volant C and Wieleczko J P 1997 *Phys. Lett.* B **390** 41

[5] Ma Y G, Natowitz J B, Wada R, Hagel K, Wang J, Keutgen T, Majka Z, Murray M, Qin L, Smith P, Alfaro R, Cibor J, Cinausero M, Masri Y El, Fabris D, Fioretto E, Keksis A, Lunardon M, Makeev A, Marie N, Martin E, Martinez-Davalos A, Menchaca-Rocha A, Nebbia G, Prete G, Rizzi V, Ruangma A, Shetty D V, Souliotis G, Staszel P, Veselsky M, Viesti G, Winchester E M and Yennello S J 2005 *Phys. Rev.* C **71** 054606

[6] Ma Y G 2000 *Acta Phys. Sin.* **49** 654 (in Chinese)

[7] Hauger J A, Warren P, Albergo S, Bieser F, Brady F P, Caccia Z, Cebra D A, Chacon A D, Chance J L, Choi Y, Costa S, Elliott J B, Gilkes M L, Hirsch A S, Hjort E L, Insolia A, Justice M, Keane D, Choi Y, Costa S, Elliott J B, Gilkes M L, Hirsch A S, Hjort E L, Insolia A, Justice M, Keane D, Kintner J C, Lindenstruth V, Lisa M A, Matis H S, McMahan M, McParland C, Muller W F J, Olson D L, Partlan M D, Porile N T, Potenza R, Rai G, Rasmussen J, Ritter H G, Romanski J, Romero J L, Russo G V, Sann H, Scharenberg R P, Scott A, Shao Y, Srivastava E B K, Symons T J M, Tincknell M, Tuve C, Wang S, Wieman H H, Wienold T and Wolf K 1998 *Phys. Rev.* C **57** 764

[8] Tsang M B, Friedman W A, Gelbke C K, Lynch W G, Verde G and Xu H 2001 *Phys. Rev.* C **64** 041603

[9] Chen L W, Greco, Ko C M and Li B A 2003 *Phys. Rev. Lett.* **90** 162701

[10] Zhong C, Ma Y G, Fang D Q, Cai X Z, Chen J G, Shen W Q, Tian W D, Wang K, Wei Y B, Chen J H, Guo W, Ma C W, Ma G L, Su Q M, Yan T Z and Zuo J X 2006 *Chin. Phys.* **15** 1481

[11] Ma Y G, Yan T Z, Cai X Z, Chen J G, Fang D Q, Guo W, Liu G H, Ma C W, Ma E J, Shen W Q, Shi Y, Su Q M, Tian W D, Wang H W and Wang K 2007 *Nucl. Phys.* A **787** 611c

[12] Yan T Z, Ma Y G, Cai X Z, Fang D Q, Guo W, Ma C W, Shen W Q, Tian W D and Wang K 2007 *Chin. Phys.* **16** 2676

[13] Li B A, Chen L W and Ko C M 2008 *Phys. Rep.* **464** 113

[14] Ma C W, Fu Y, Fang D Q, Ma Y G, Cai X Z, Guo W, Tian W D and Wang H W 2008 *Chin. Phys.* B **17** 1214

[15] Ma Y G, Su Q M, Shen W Q, Han D D, Wang J S, Cai X Z, Fang D Q and Zhang H Y 1999 *Phys. Rev.* C **60** 024607

[16] Dempsey J F, Charity R J, Sobotka L G, Kunde G J, Gaff S, Gelbke C K, Glasmacher T, Huang M J, Lemmon R C, Lynch W G, Manduci L, Martin L, Tsang M B, Agnihotri D K, Djerroud B, Schroder W U, Skulski W, Toke J and Friedman W A 1996 *Phys. Rev.* C **54** 1710

[17] Li B A, Ren Z, Ko C M and Yennello J 1996 *Phys. Rev. Lett.* **76** 4492

[18] Pak R, Benenson W, Bjarki O, Brown J A, Hannuschke S A, Lacey R A, Li B A, Nadasen A, Norbeck E, Pogodin P, Russ D E, Steiner M, Stone N B, Molen A M V, Westfall G D, Yang L B and Yennello S J 1997 *Phys. Rev. Lett.* **78** 1022

[19] Pak R, Li B A, Benenson W, Bjarki O, Brown J A, Hannuschke S A, Lacey R A, Magestro D J, Nadasen A, Norbeck E, Russ D E, Steiner M, Stone N T B, Molen A M V, Westfall G D, Yang L B and Yennello S J 1997 *Phys. Rev. Lett.* **78** 1026

[20] Chen L W, Zhang F S and Jin G M 1998 *Phys. Rev.* C **58** 2283

[21] Kumar S, Sharma M K, Prui R K, Singh K P and Govil I M 1998 *Phys. Rev.* C **58** 3494

[22] Miller M L, Bjarki O, Magestro D J, Pak R, Stone N T B, Tonjes M B, Molen A M V and Westfall G D 1999 *Phys. Rev. Lett.* **82** 1399

[23] Fang D Q, Shen W Q, Feng J, Cai X Z, Wang J S, Su Q M, Ma Y G, Zhu Y T, Li S L, Wu H Y, Gou Q B, Jin G M, Zhan W L, Guo Z Y and Xiao G Q 2000 *Phys. Rev.* C **61** 044610

[24] Fang D Q, Shen W Q, Feng J, Cai X Z, Wang J S, Su Q M, Ma Y G, Zhu Y T, Li S L, Wu H Y, Gou Q B, Jin G M, Zhan W L, Guo Z Y and Xiao G Q 2000 *Chin. Phys. Lett.* **17** 267

[25] Fang D Q, Shen W Q, Feng J, Cai X Z, Ma Y G, Zhang H Y, Hu P Y, Zhan W L, Guo Z Y, Xiao G Q, Li J X, Wang M, Wang J F, Ning Z J, Wang J Q, Wang J S, Wang Q J and Chen Z Q 2001 *Eur. Phys. J.* A **10** 381

[26] Mocko M, Tsang M B, Andronenko L, Andronenko M, Delaunay F, Famiano M, Ginter T, Henzl V, Henzlova D, Hua H, Lukyanov S, Lynch W G, Rogers A M, Steiner M, Stolz A, Tarasov O, van Goethem M J, Verde G, Wallace W S and Zalessov A 2006 *Phys. Rev.* C **74** 054612

[27] Mocko M, Tsang M B, Lacroix D, Ono A, Danielewicz P, Lynch W G and Charity R J 2008 *Phys. Rev.* C **78** 024612

[28] Brohm T and Schmidt K H 1994 *Nucl. Phys.* A **569** 821

[29] Fang D Q, Feng J, Shen W Q, Cai X Z, Wang J S, Ye W and Ma Y G 1999 *High Energy Phys. Nucl. Phys.* **23** 475 (in Chinese)

[30] Zhong C, Ma Y G, Fang D Q, Cai X Z, Chen J G, Shen W Q, Tian W D, Wang K, Wei Y B, Chen J H, Guo W, Ma C W, Ma G L, Su Q M, Yan T Z and Zuo J X 2006 *Chin. Phys.* **15** 1481

[31] Zhong C, Fang D Q, Cai X Z, Shen W Q, Zhang H Y, Wei Y B and Ma Y G 2003 *High Energy Phys. Nucl. Phys.* **27** 39 (in Chinese)

[32] Eisenberg Y 1954 *Phys. Rev.* **52** 1378

[33] Gaimard J J and Schmidt K H 1991 *Nucl. Phys.* A **531** 709